

Viewpoint pubs.acs.org/macroletters

100th Anniversary of Macromolecular Science Viewpoint: High Refractive Index Polymers from Elemental Sulfur for Infrared Thermal Imaging and Optics

Tristan S. Kleine, Richard S. Glass, Dennis L. Lichtenberger, Michael E. Mackay, Kookheon Char, Robert A. Norwood,* and Jeffrey Pyun*



Cite This: ACS Macro Lett. 2020, 9, 245-259



ACCESS

Metrics & More

Sulfur ↔ Inverse Vulcanization ↔ IR Imaging

Article Recommendations

ABSTRACT: Optical technologies in the midwave and long wave infrared spectrum (MWIR, LWIR) are important systems for high resolution thermal imaging in near, or complete darkness. While IR thermal imaging has been extensively utilized in the defense sector, application of this technology is being driven toward emerging consumer markets and transportation. In this viewpoint, we review the field of IR thermal imaging and discuss the emerging use of synthetic organic and hybrid polymers as novel IR transmissive materials for this



Chalcogenide Hybrid Inorganic/Organic Polymers

application. In particular, we review the critical role of elemental sulfur as a novel feedstock to prepare high refractive index polymers via inverse vulcanization and discuss the fundamental chemical insights required to impart improved IR transparency into these polymeric materials.

S ince the discovery of infrared (IR) irradiation by Herschel in 1800¹ and the development of IR thermal radiation laws by Planck in 1900,² IR optics have evolved into important methodologies for a number of technologies, which include IR spectroscopy for the chemical identification of molecular compounds and IR thermal imaging systems.3 IR imaging systems operating across a broad range of the infrared spectrum $(1-14 \mu m)$ offer distinct advantages for noninvasive, high resolution detection of people and objects in the absence of visible light. IR thermal imaging has been widely deployed for military applications, but there has been strong interest to apply these systems to consumer products for smartphones, portable electronics, transportation, and other emerging markets.

IR imaging systems are generally more expensive than those operating at visible wavelengths, which has ultimately limited the widespread use of IR cameras for nondefense related markets, where camera costs remain prohibitive for high volume deployment. A significant fraction of the high cost for IR imaging systems arises from the nearly exclusive use of expensive inorganic transmissive materials for IR lenses and windows, such as germanium (Ge) or chalcogenide glasses (ChGs). Conventional transmissive materials used in imaging applications, such as metal oxide glasses or organic polymers, typically possess intrinsic fundamental vibrations and overtones at the IR wavelengths of interest. Synthetic organic polymers are also generally composed of low refractive index organic monomers that have further stifled the use of these materials as IR transmissive optical elements. However, polymers offer numerous other advantages over Ge or ChGs, which include low cost, facile processing into optical elements and broad chemical diversity, all of which have spurred recent interest in the development of synthetic polymers for IR applications.

A major breakthrough in this area was achieved by Pyun et al. in 2013 with the concept of copolymerizing elemental sulfur with organic comonomers via a process termed, inverse vulcanization, 4-6 which afforded hybrid polymers of chalcogenide and organic comonomer units. These hybrid polymers, subsequently termed Chalcogenide Hybrid Inorganic/Organic Polymers (CHIPs), were first demonstrated as midwave infrared (MWIR) transmissive materials in 2014 and exhibited both a high refractive index and improved IR transparency relative to conventional plastics. This discovery by Pyun and co-workers at the University of Arizona, Seoul National University, and the University of Delaware has spawned significant interest in other research groups around the world, notably from the U.S. Naval Research Laboratories. Herein, we review for the first time, the historical development of this new class of IR optical polymers, along with the challenges of developing proper protocols for the synthesis and optical characterization of these novel transmissive materials, particularly for new frontiers in long wave infrared (LWIR) imaging. A short introductory background to IR imaging and IR

Received: December 3, 2019 Accepted: January 29, 2020



transmissive materials is also included to provide context for the recent advances in IR optical polymers.

Types of IR imaging systems: SWIR, MWIR, and LWIR: The different regions of the infrared spectrum have been defined based on terrestrial atmospheric absorptions from water, ozone, and carbon dioxide, where the windows between major absorptions delineate different regions of the IR. The first region is referred to as the short wave IR (SWIR, $1-3 \mu m$) and can be a major component of reflected light. Longer wavelengths of infrared light, commonly referred to as the mid-IR or "thermal IR" refers to photons emitted from blackbody radiators. The spectrum and intensity of this light can be correlated to the temperature of the blackbody through Planck's law and is the basis for certain applications of IR imaging (namely, IR thermography). Information about chemical composition of materials is also contained in the thermal IR spectrum. The thermal IR is further segregated into the midwave infrared (MWIR, $3-5 \mu m$) and long-wave infrared (LWIR, 7-14 μ m) given the strong absorptions of water molecules from $\sim 5-7.5 \, \mu \text{m}$ and absorptions from CO₂ dominating beyond 14 μ m (Figure 1a). This nomenclature

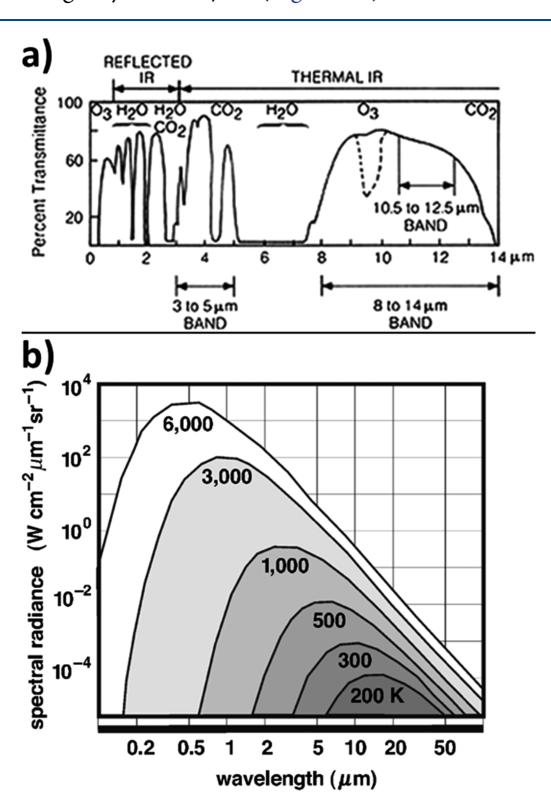


Figure 1. (a) Atmospheric windows in visible and infrared regions. Reproduced with permission from ref 8. Copyright 2017 Springer Nature. (b) Planck curves of a blackbody (after Flir, 2000) at different temperatures (in degrees Kelvin). Ordinate, spectral radiance [W cm $^{-2}$ μ m $^{-1}$ sr $^{-1}$]; abscissa, wavelength in micrometers. Reproduced with permission from ref 10. Copyright 2003 Springer Nature.

system is useful when discussing IR imaging systems since optical elements and detectors vary depending on the IR spectral window of interest. Together, these features make imaging in the MWIR and LWIR highly versatile and, consequently, the main focus of this Review regarding application to polymeric transmissive materials.

SWIR imaging has been primarily used in low light conditions and takes advantage of avalanche photodiodes or

near IR (NIR) illumination 10 to increase contrast under semidark conditions. From an imaging standpoint, moving to longer IR wavelengths offers distinct advantages over the SWIR with respect to identifying and analyzing certain imaging targets as previously mentioned. For instance, IR thermography can be used to determine the temperature of an object remotely and has been demonstrated in a variety of applications to rapidly assess otherwise difficult to probe environments. Nonmilitary applications of IR thermography range from monitoring breast cancer¹¹ and other biological disease states, ^{12,13} to analysis of building infrastructure ^{14,15} and continuous monitoring of machinery. 16 IR thermal imaging is also heavily used in the electronics industry as a rapid assessment tool for identifying thermal abnormalities in electrical systems indicative of defects and consequently impending failure. 17,18 An important consideration in IR thermography is that, depending on the temperature of the blackbody being interrogated, different regimes of the infrared are more suitable for this technique, as is illustrated in Figure 1b. The Planck curves shown in Figure 1b demonstrate the relationship between temperature of a blackbody and the corresponding wavelength range and total spectral irradiance emitted. The lower the equilibrium temperature of a blackbody radiator, the narrower the spectrum of emitted photons is, and a red shifting of the wavelength of highest irradiance is observed. For example, the 300 K Planck curve (approximately the temperature of a human) illustrates that peak intensity of radiated photons are centered at $\sim 10 \ \mu m$ in the IR spectrum. This is, in part, what makes LWIR imaging of particular interest for monitoring human subjects. Furthermore, in general, lower sensitivity is required when attempting to measure objects at wavelengths closer to their peak intensity; 1 thus, for relatively lower temperature objects (Figure 1b), imaging in the LWIR is in principle more appropriate, but detection technology choices must also be considered. In addition to the varied uses of IR thermography, IR imaging can be applied to hyperspectral imaging, a technique that maps a defined portion of the electromagnetic spectrum to each pixel in a detector providing spectral and spatial information,²⁴ which allows for stand-off chemical detection/identification and is of unique interest for detecting explosives, $^{21-24}$ as well as geological mapping from space. 25,26 These unique applications of IR imaging are some of the driving forces for the development of this field but have not realized widespread use given the high cost of such systems, motivating the need to reduce the cost of each component as much as possible.

Imaging in the MWIR is particularly costly due to the detectors used at these wavelengths. These are primarily quantum detectors (i.e., photodiodes) and work essentially like a photovoltaic, whereby absorption of IR photons and separation of charge leads to the generation of current that is interpreted as an electronic signal/response.²⁷ The mercury/ cadmium/telluride (MCT) alloys are commonly used for this application, as the band gap of MCT can be tuned over both the MWIR and LWIR by adjusting alloy composition, thus, making it a versatile detector material.²⁸ However, this technology requires a cooling system (Peltier thermoelectric cooling or use of cryogenic liquids) to be integrated into the detector due to the lower energies of IR photons in order to reduce background noise (dark current), which ultimately raises the cost of these systems.²⁹ By the same token, these detectors are highly sensitive and impart sharper contrast in the MWIR versus LWIR imaging, 30 which warrants the

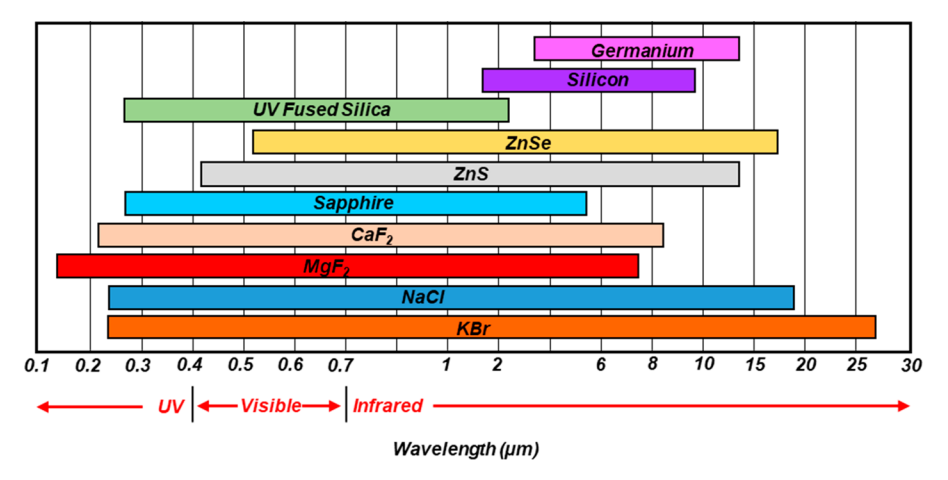


Figure 2. Transparency windows for various optical materials throughout the visible and infrared regions of the electromagnetic spectrum (Edmund Optics).

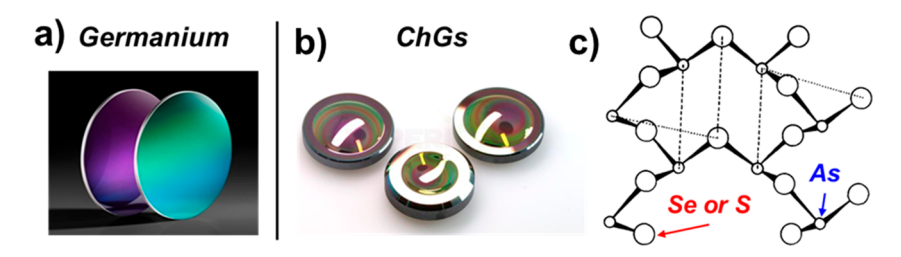


Figure 3. Examples of materials used for LWIR imaging: (a) germanium (Hyperion Optics) and (b) chalcogenide glasses (Edmunds Optics Inc.). (c) Part of a single sheet in the orpiment structure (of As_2S_3) viewed along the b_0 axis. Large circles are sulfur and small circles are arsenic atoms. Broken lines indicate the 4.22 Å, c_0 translation distance between like atoms, and dotted lines indicate the 4.24 Å distance between unlike atoms; As_2Se_3 is closely related to this structure, and it has been proposed that the As_2S_3 glass exists as disordered sheets with similar bond lengths to the crystal. 49 Adapted with permission from ref 49. Copyright 1974 Elsevier.

incurred cost under certain circumstances, namely, in defense applications where imaging performance supersedes cost considerations.³¹

Development of uncooled IR cameras enabling wide scale deployment was sought by the military in the 1970s, leading to Honeywell developing the favored technology known as microbolometers. 32,33 As opposed to the quantum detectors described earlier, microbolometers function by a response to IR-induced heating of the sensor material. Electronic signal generation is based on changes in resistance across a LWIR absorbing material (now, most commonly, vanadium oxide, although other materials have been explored)³⁴ as a consequence of IR heating, where temperature change and, hence, resistance are proportional to the number of impinging IR photons.³⁵ Each pixel in a microbolometer is thermally insulated enabling fabrication of high resolution focal plane arrays with pitch sizes on the order of 10s of microns and has proven to be an invaluable design for IR cameras.²⁷ While microbolometers have brought the cost of such systems down, other technologies are still being investigated with the aim of improving performance and further reduced cost.³⁶ Access to cheap and compact LWIR cameras has enabled improved imaging and diagnostics of humans as previously mentioned and is also of great interest for aiding in Advanced Driver Assist Systems (ADAS), as well as completely autonomous vehicles, 3,37-40 since LWIR imaging is particularly relevant for applications where lower cost and identification of humans are primary concerns.

IR transmissive materials: Historically, a wide range of materials have been used for IR spectroscopic and thermal

imaging applications which include metal fluorides (e.g., LiF, MgF₂, BaF₂), inorganic salts (e.g., NaCl, KBr), semiconductor materials (e.g., Ge, Si, CdTe, GaAs, ZnSe, or ZnS), and ChGs (e.g., AsSe, AsS, GeAsSe, GeSbSe; see Figure 2). As alluded to previously, IR imaging systems require the material used in the device be transparent at the wavelengths of interest, while also being amenable to processing of the raw material form into the final optical element. Consequently, semiconductors and ChGs are the materials primarily used for fabrication of IR optics, 41 since these classes of materials are chemically stable (i.e., not hygroscopic as in the case of metal fluorides), while also possessing high refractive index and excellent IR transparency. It is important to note that silica-based glasses, while being one of the most commonly used materials for optical applications, are only suitable for applications in the visible-SWIR, as optical transparency drops precipitously after around 3 μ m. While synthetic polymer products are currently not among these IR transmissive materials, we posit that advancement of this field can be served by the development of new materials for these wavelengths, specifically, low-cost IR transparent plastics.

The crystalline semiconductors typically used for IR imaging, that is, silicon, germanium, and zinc selenide/sulfide, are produced or grown through various labor intensive processes 42,43 and then further processed for use as a free-standing bulk optic. Fabrication of optical elements is typically performed by single-point diamond turning, which is a subtractive manufacturing process with computer numerical control (CNC) capabilities and is done in a serial fashion, which is neither cost-efficient nor scalable.⁴⁴

There remain clear technological needs for IR transmissive materials derived from lower cost starting materials and amenable to inexpensive processing methods for optical element fabrication to enable production of IR cameras for consumer markets (representative examples shown in Figure 3). Chalcogenide glasses (ChGs) are a possible solution to this issue, given their similar transparency to germanium at certain compositions, and are amenable to solution and melt processing, unlike crystalline semiconductor materials. Chalcogenide glasses are amorphous, polymeric network solids comprised of covalent bonds between chalcogen atoms (group 6 atoms heavier than oxygen, such as, S, Se, and Te) and more electropositive elements capable of forming networks (e.g., As and Ge, which are commonly used in IR optics/photonics applications).45 Various bulk properties of chalcogenide glasses can be tuned by adjusting the relative ratios of metal and chalcogen in the glass, or by using ternary mixtures. The caveat to this tunability requires that compositions must remain in the glass forming regime to avoid crystallization. In general, inclusion of higher molecular weight chalcogens increases refractive index (generally n > 2.0for ChGs) in binary mixtures, but at the cost of lower T_g and poorer glass forming ability. 46,47 So while As₂Te₃ glasses afford the broadest windows of transparency for binary arsenic glasses, the poor mechanical properties make selenide glasses or ternary ChGs (which exhibit broader glass forming regimes) the more attractive ChG materials for IR imaging.

The rheological properties of ChGs make them amenable to melt processing⁴¹ and were first demonstrated for high precision molding of ChG optics in 2003 as viable, cost-effective alternatives to Ge. 38 Since ChGs are amorphous materials with glass transition temperatures widely ranging from below 0 °C to as high as ~400 °C, depending on composition⁵⁰ (for glasses particularly relevant to IR optics), can be thermomechanically reformed in much the same way plastics are. A downside to the use of ChGs in IR optics is the low Earth abundance and high cost of the raw materials, coupled with toxicity concerns of end of life products. Two of the metals commonly alloyed with chalcogens for IR optics (i.e., arsenic and germanium) are only produced in certain regions of the world, which sharply affects supply and accessibility of these critical materials. It is worth noting that Ge has been identified as a critical element in the United States Geological Survey Mineral Commodities Summary (2019), which has profound implications for defense and national security of numerous countries due to the use of Ge for optical military applications.⁵¹ Additionally, the synthesis of ChGs requires highly refined starting materials free of contaminants and employs a number of high-temperature processes to synthesize and purify the glass, which is critical for high performance in optical fibers where impurities result in significant absorption losses. 52-54 Chalcogenide glasses may also be solution-processed in aqueous base solutions⁵⁵ or short chain alkyl amines (propyl/butyl amine), with mixtures of amines and thiols being required to dissolve the selenide-containing ChGs. 56-59 While solutions of ChGs have successfully been used to inkjet-print micro-optics, it should be noted that handling of ChG solutions must be performed under an inert atmosphere and in the absence of water, requiring the use of glove boxes. 55 Given these considerations, a polymeric-based material would potentially offer the same benefits in terms of ease of processablility, without the use of costly raw materials.

IR transparent plastics: Crystalline and noncrystalline (ChG) semiconductors have become the standard transmissive materials of choice for IR optics because of desirable optical properties arising from the nature of their constituent atoms. Specifically, the large mass of the atoms found in these materials shift the vibrational energies of these bonds to outside the MWIR (3–5 μ m) and LWIR (7–14 μ m) spectral windows. Refractive indices for these materials are also typically very high (n > 2.0), again due to the presence of large, highly polarizable atoms. The use of conventional polymeric materials for IR optics would presumably be precluded by the presence of a large volume fraction of C–C, C–H, and other C–X heteroatom covalent bonds in the macromolecular framework. This intrinsic limitation is illustrated in Figure 4 for the FTIR spectra of polystyrene

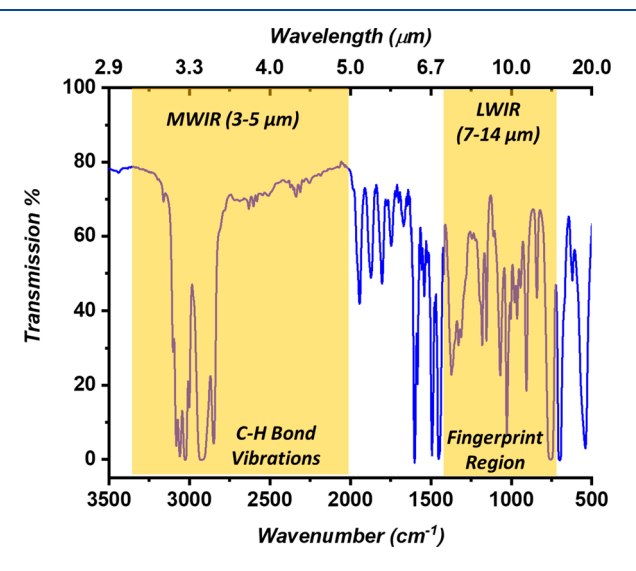


Figure 4. FTIR spectrum of polystyrene film denoting the MWIR and LWIR bands and the nature of the vibrations responsible for opacity in these regions

with MWIR and LWIR bands highlighted in yellow. Absorptions in the MWIR are dominated by C-H stretching vibrations at ~3000 cm⁻¹. Hence, the guiding principle in the design of MWIR transparent plastics is the omission of C-H moieties in the material without sacrificing other desirable material properties. While the chemical design principles for MWIR transparency in polymers can be reduced to practice (removing C-H content), similar approaches for LWIR transparency are profoundly more complex due to the abundance of vibrational absorptions in this spectral window for organic-based materials. Despite these significant challenges, the advantages of polymeric materials for this application, as previously discussed, warrant fundamental research into the synthesis and characterization of IR transmissive polymers. Organic polymers based on aliphatic units, such as polyethylene or norbornene-olefinic copolymers (i.e., Topas), possess fairly simple fingerprint region spectra and, hence, have been used as thin LWIR barrier coatings. 60 However, the low refractive index of these polymers (and organic polymers in general) would require thicker optical elements where transmission becomes an issue, although elegant design solutions have been shown to circumvent both issues to some degree.⁶¹

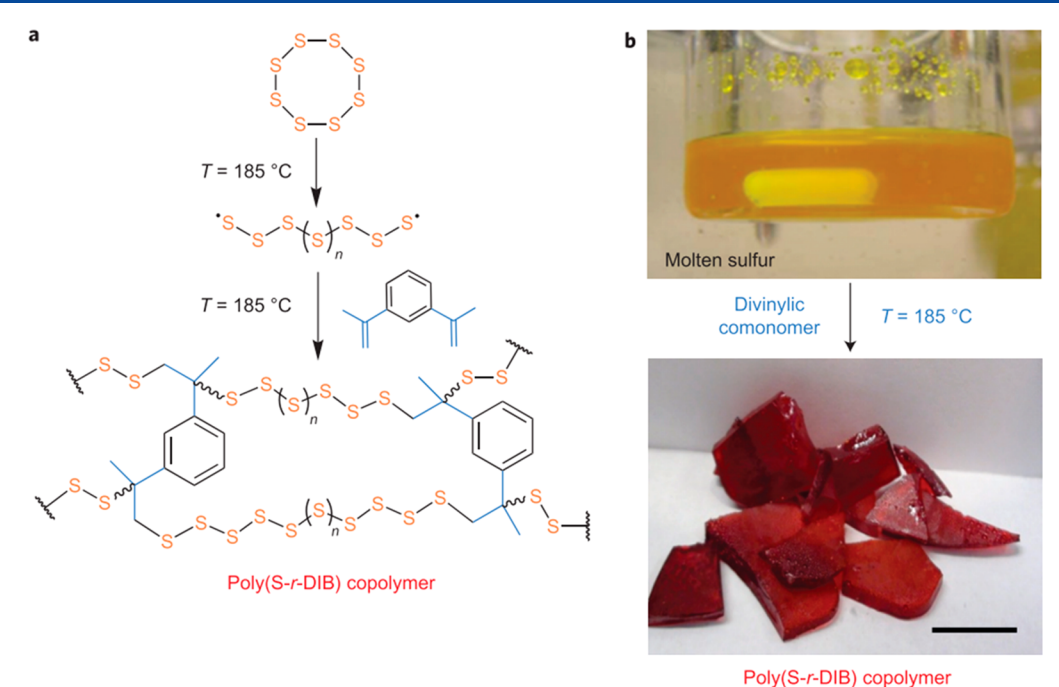


Figure 5. (a) Synthetic scheme for the copolymerization of S_8 with DIB to form chemically stable sulfur copolymers. (b) Images of liquid sulfur and poly(S-r-DIB) glass with 30 wt % DIB (scale bar, 2 cm). The key feature of this synthetic method is the direct use of liquid sulfur as both the solvent and the comonomer, along with DIB, to form chemically stable glassy copolymers. Reproduced with permission from ref 62. Copyright 2013 Nature Publishing Group.

To this end, Pyun and co-workers have developed a new class of materials termed Chalcogenide Hybrid Inorganic/Organic Polymers (CHIPs), which are copolymers of chalcogens and organic monomers. These materials feature a high chalcogen content and, thus, possess desirable bulk properties, such as high refractive index and IR transparency, while maintaining the melt and solution processability associated with conventional thermoplastic polymers. The application of CHIPs to IR imaging is a new advance, but represents an important first step in replacing semiconductor materials for this application.

Polymerization with elemental sulfur: A major breakthrough in the synthesis of IR optical thermoplastics and thermosets of high refractive index (n = 1.7-2.1) was the development of a process termed inverse vulcanization, where molten sulfur, acting as a solvent and monomer, was copolymerized with 1,3-diisopropenylbenzene (DIB) to prepare a chemically stable and processable sulfur plastic (Figure 5).⁶² This process is a bulk free radical copolymerization conducted in molten sulfur that operates at temperatures in the range of T = 130-185 °C, which is significantly lower than the temperatures required for Ge or ChG fabrication. These materials are intriguing for IR optics, since the S-S bonds in the copolymer are largely IR inactive in the MWIR and LWIR regime, while also imparting high n to the macromolecule. Since the initial report on the inverse vulcanization process in 2013, a wider class of organic comonomers have been investigated, which now include alkenes, 63-68 alkynes, 69,70 naturally occurring olefins, 71-78 allyl ethers, 79-81 oleyamine, 82 maleimides, 83 and benzoxazines.84,85

Midwave-infrared imaging: IR imaging through CHIPs was demonstrated in 2014 along with further exploration of the optical properties of CHIPs. The refractive indices of CHIPs are significantly higher than conventional organic polymers

(Figure 6), or classical high refractive index polymers (HRIPs) which usually fall below n = 1.8.87 The inverse vulcanization process afforded an unusually large volume fraction of highly polarizable sulfur units and was the basis for the inherently high refractive indices observed in CHIPs materials. Furthermore, refractive indices of CHIPs materials were found to track with chalcogen content as expected and were found to be as high as n = 1.865 when 80 wt % sulfur was used in the copolymerization. Compositions containing less than 20 wt % organic cross-linker are generally not investigated for optical applications since a low organic content generally resulted in poor thermomechanical properties and reduced solubility. The high sulfur content of CHIPs also afforded a large fraction of the chemical bonds in the polymer to be comprised of polysulfide bonds, which is the chemical origin for the improved MWIR transparency of CHIPs materials. To illustrate this fact, poly(methyl methacrylate) (PMMA) and CHIPs windows of similar thicknesses were placed in front of a MWIR camera (operating at 3-5 μ m), and a human subject was imaged through both windows (Figure 6d,e). The image of the human subject was significantly obscured when viewed through the PMMA window, but could clearly be seen when replaced with the CHIPs window. Various optical elements demonstrated in this report (windows and lenses) were fabricated from melt processing with simple PDMS replicas and illustrated the processing advantages of CHIPs in comparison to semiconductors typically used for IR imaging. This report was the first step in demonstrating the possibility of using low cost, easily processable organic polymers for IR imaging and paved the way for this new field.

Improving thermomechanical properties: One drawback to CHIPs limiting their widespread implementation in IR imaging systems is their inferior thermomechanical properties relative to conventional optical polymers (e.g., PMMA), which is manifested in bulk properties, such as the glass transition

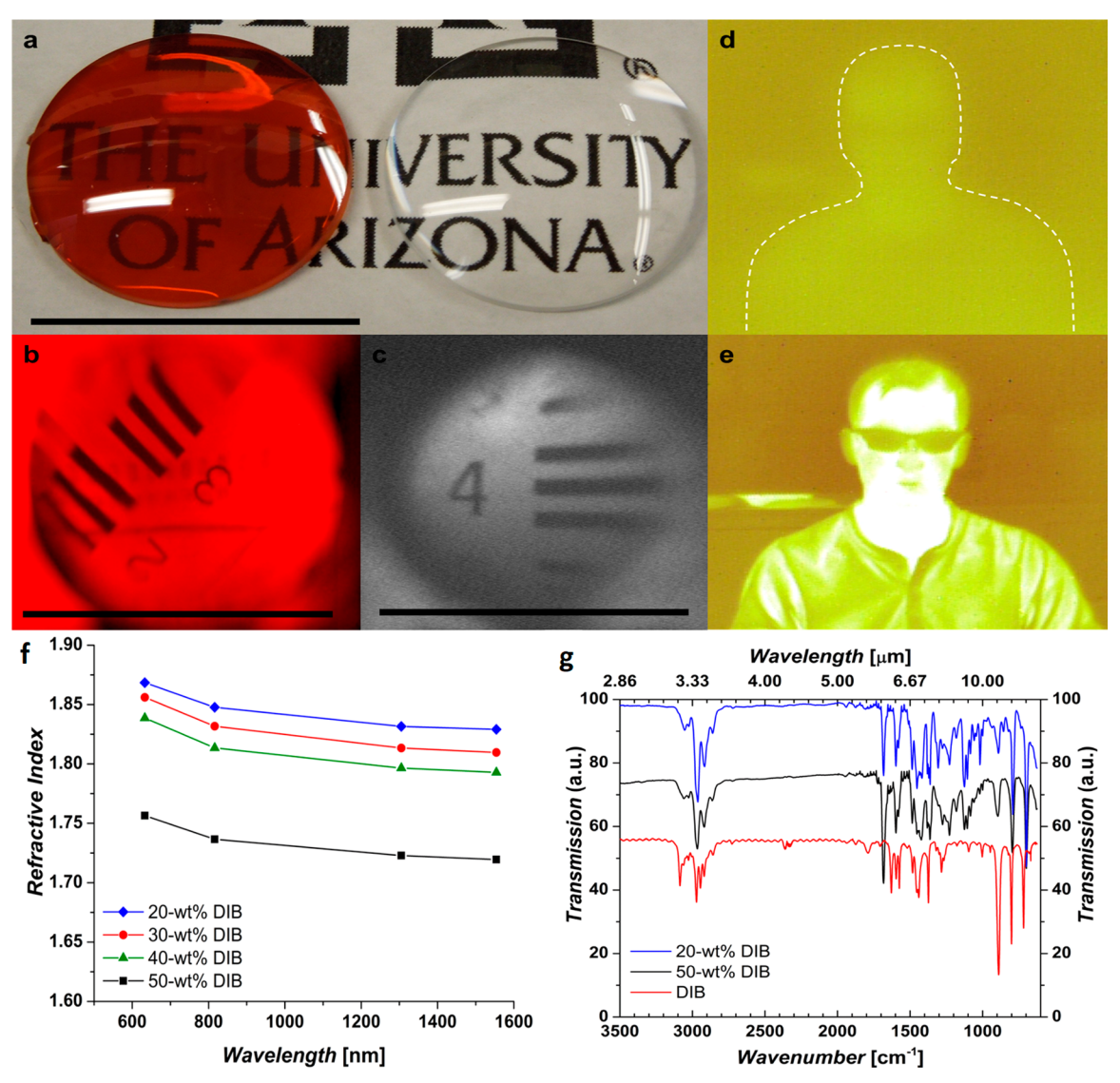


Figure 6. (a) Digital image of lenses (left) poly(S-r-DIB) copolymer (80 wt % S_8) and (right) glass, (b) digital image of a USAF target through copolymer lens in visible wavelengths, and (c) an image captured with a near-infrared camera of the USAF target illuminated with a 1550 nm laser (scale bars = 25.4 mm). (d) Thermal imaging of human subject through PMMA film (\sim 1 mm) in the mid-IR (3–5 μ m) regime (dotted white line highlights the area where the subject is sitting); (e) thermal imaging of a human subject through 80 wt % S_8 poly(S-r-DIB) copolymer film (\sim 1 mm) in the mid-IR (3–5 μ m) regime (images are false colored Sepia tone: white corresponds to \sim 37 °C and brown corresponds to \sim 24 °C). (f) Refractive indices vs wavelength as a function of poly(S-r-DIB) copolymer composition for 200 μ m films; results are the average of values for light polarized parallel and perpendicular to the film surface; (g) stacked transmission FTIR spectrum (arbitrary transmission units) comparing poly(S-r-DIB) copolymers (20 wt % DIB (top spectrum); 50 wt % DIB (middle spectrum)) to pure 1,3-di-isopropenylbenzene comonomer (bottom spectrum). Adapted with permission from ref 86. Copyright 2014 John Wiley & Sons. Logo courtesy of the University of Arizona.

temperature $(T_{\rm g})$ of the material. We observed a seemingly mutually exclusive trend in the desirable properties of CHIPs, where high sulfur content compositions were needed to impart high n and IR transparency, but also lowered the $T_{\rm g}$ and mechanical properties of these materials. A key technical question was whether appropriate design of the organic comonomer could be exploited to improve thermomechanical properties, despite being the minority component in the final CHIPs optical element. It is well-known that increasing the crosslink density of polymer networks can increase the $T_{\rm g}$ of a polymeric material, and this feature was leveraged by the synthesis of new organic comonomers for CHIPs. A trifunctional analogue of DIB (1,3,5-tri-isopropenylbenzene (TIB)) was synthesized by efficient Suzuki cross-coupling of 1,3,5-tribromobenzene and isopropenylboronic acid pinacol ester

followed by inverse vulcanization with sulfur to afford poly(sulfur-random-1,3,5-tri-isopropenylbenzene) (poly(S-r-TIB)). This material was observed to be a thermoset using rheological characterization and a significant increase in $T_{\rm g}$ was observed with higher compositions of TIB, enabling tunability of the $T_{\rm g}$ s from 68 to 130 °C. The utility of the enhanced thermomechanical properties of poly(S-r-TIB) was demonstrated by a laser damage study, where a laser photodiode operating at 405 nm (which is an optically absorbing wavelength for the CHIPs materials) was focused on windows of poly(S-r-TIB) and poly(S-r-DIB). In these studies, poly(S-r-DIB) windows showed significant laser-induced heating and damage within 5 s of irradiation, while the poly(S-r-TIB) window maintained structural integrity, which pointed to the improved thermal properties of this copolymer. Deformation

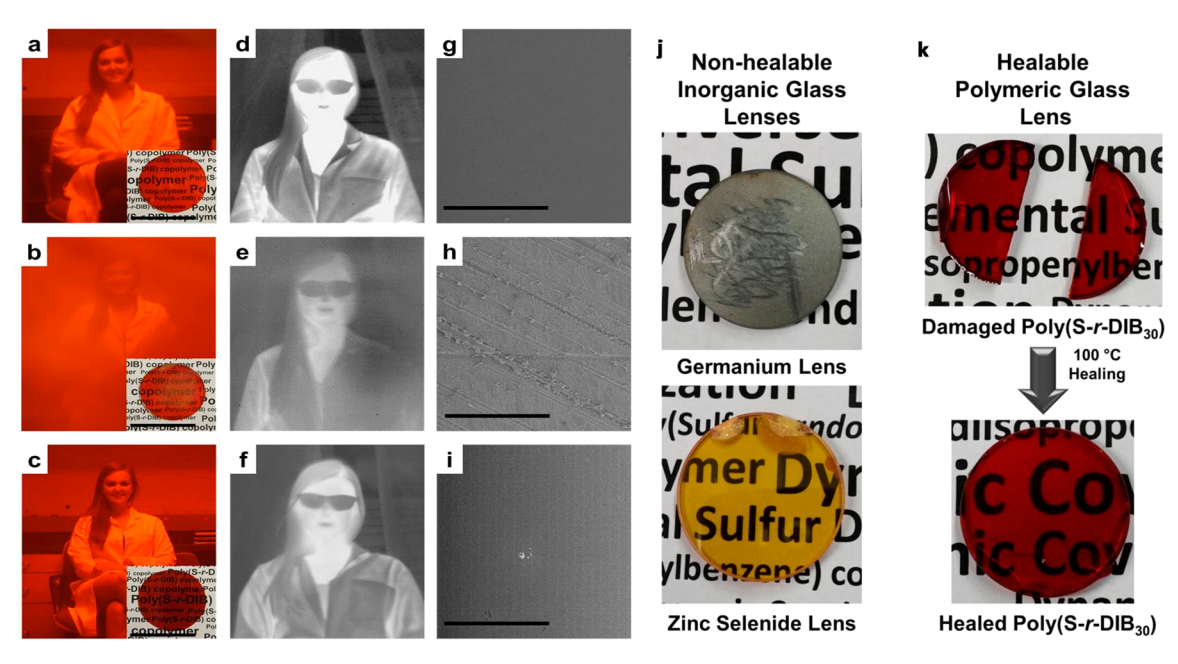


Figure 7. (a–c) Digital visible wavelength images captured through poly(S-r-DIB₃₀) copolymer window of a female subject: (a) pristine window; (b) damaged window; (c) self-healed window. Insets: Digital images of windows over printed text. (d–f) Digital, mid-infrared wavelength (3–5 μ m) images captured through poly(S-r-DIB₃₀) copolymer window of a female subject: (d) pristine window; (e) damaged window; (f) self-healed window. (g–i) Environmental scanning electron microscopy (e-SEM) images of poly(S-r-DIB₃₀) copolymer window surface: (g) pristine window; (h) damaged window; (i) self-healed window. Scale bars for insets in (a)–(c) are 5.5 cm and for (g)–(i) are 300 μ m. (j) Damaged inorganic lenses (germanium lens (top) and zinc selenide lens (bottom)) that cannot be repaired for IR imaging. (k) Poly(S-r-DIB₃₀) copolymer lens which is drastically damaged but repaired and functional by thermal annealing at 100 °C. Adapted with permission from ref 91. Copyright 2015 American Chemical Society.

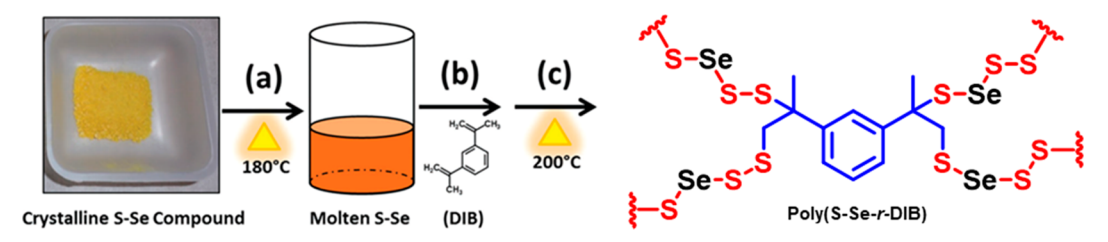


Figure 8. Flow diagram of poly(S–Se-*r*-DIB) polymer fabrication. (a) melt and stir S–Se crystalline compound. (b) Add DIB and continue stirring. (c) Pour molten material into a mold (e.g., a Petri dish), heat to 200 °C (1 h), and then cool to vitrify, affording poly(S–Se-*r*-DIB). Adapted with permission from ref 94. Copyright 2017 The Royal Society of Chemistry.

of optical elements handling high power laser sources is a known and studied issue, ⁸⁹ which for IR applications would require transmissive polymeric materials with improved thermomechanical properties.

Dynamic covalent CHIPs and scratch healable lenses: Another interesting property with regards to CHIPs materials is that the polysulfide network allows the material to reheal through activation of the dynamic S-S bonds^{90,91} (Figure 7). Thermal IR lenses and windows fabricated from germanium or metal chalcogenides (e.g., ZnSe) are rendered unusable for imaging after minor scratches or defects are incurred (see Figure 7j for examples) unless significant and costly processes are employed. Conversely, the use of an optical polymer possessing dynamic covalent bonds enables healing of these types of defects and reuse of damaged lenses/windows (windows in this context will refer to a flat freestanding panel of the material). Optical elements fabricated from CHIPs were easily repaired by annealing at low temperature (100 °C, Figure 7a-i) through thermolytic scission of S-S bonds to reform the copolymer network. This feature had previously been demonstrated with poly(S-r-DIB), but was found to hold

true for poly(S-r-TIB) as well, despite poly(S-r-TIB) being more densely cross-linked.

Improving refractive index in CHIPs: While the refractive indices of these first generation CHIPs materials were notably higher than most organic polymers, they are still lower than other transmissive materials typically used for IR imaging which can be as high as $n \sim 4.0$ in the case of Ge. Hence, the incorporation of selenium comonomer units into CHIPs were targeted, since elemental selenium exhibits a high refractive index (n = 2.78) and were known to bond efficiently with sulfur atoms. Unfortunately, and unlike for elemental sulfur, the floor temperature for Se₈ to polymeric selenium (i.e., gray selenium, which is highly intractable) is below the melting point of the monomeric Se, thus, precluding facile copolymerization with organic comonomers.

The first demonstration to incorporate Se into CHIPs was reported by Boyd et al. from the U.S. Naval Research Laboratory, ⁹⁴ where a multistep process was used to prepare mixed chalcogen precursors $(S_{90}Se_{10})$ for the inverse vulcanization process with DIB to afford selenium-containing terpolymers (Figure 8). This synthetic method appeared to

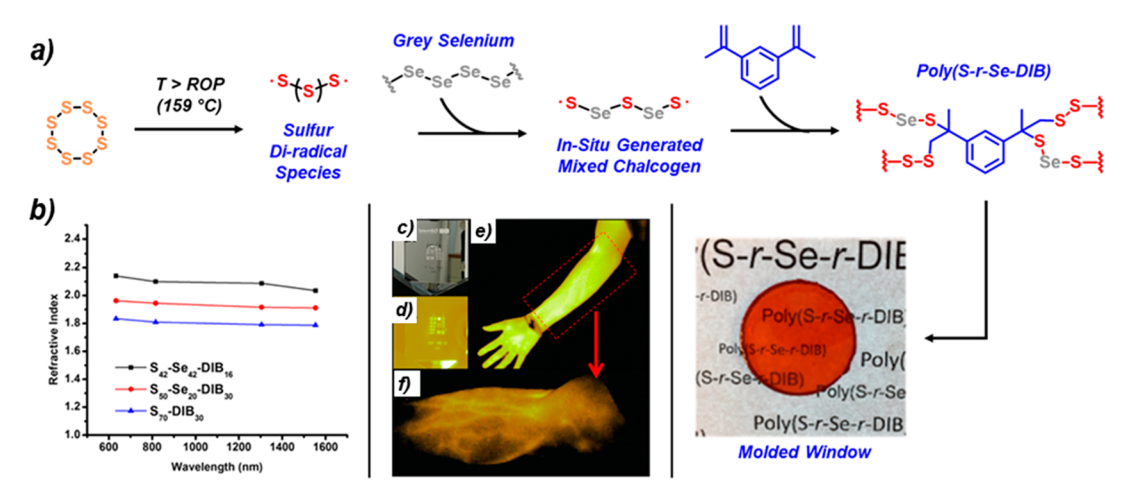


Figure 9. (a) Scheme for the synthesis of poly(S-r-Se-r-DIB); (b) refractive indices of poly(S-r-Se-r-DIB) terpolymers of varying composition vs wavelength; (c) digital image of a USAF target (purchased from Edmund Optics); images captured with a mid-IR camera, operating at 3–5 μ m, through a poly(S₅₀-r-Se₂₀-r-DIB₃₀) panel (1 mm thick, 25 mm wide) of (d) a USAF target, transparent at 3–4 μ m, (e) IR thermal image of human arm, and (f) higher resolution image of human forearm. Adapted with permission from ref 95. Copyright 2017 American Chemical Society.

be limited with respect to preparing higher Se content terpolymers. Furthermore, optical characterization of these materials with respect to the refractive index and IR transmissive properties was not fully explored. The authors termed these chalcogenide hybrid polymers, "Organically Modified Chalcogenides" or ORMOCHALCs.

Independently, the Pyun group reported on the direct addition of polymeric Se (i.e., gray selenium) to the inverse vulcanization process, where a one-pot terpolymerization of S_8 , gray Se and DIB to form poly(sulfur-random-selenium-random-1,3-di-isopropenylbenzene) (poly(S-r-Se-r-DIB)) CHIPs (Figure 9).95 The key finding in this study was the use of liquid sulfur radical species to "crack" and react with gray selenium to form soluble mixed S-Se oligomers that copolymerized with DIB at reduced temperatures (T = 160 °C; Figure 9a). The inverse vulcanization approach afforded high selenium loadings that afforded the highest refractive index of any synthetic polymer to date ($n \le 2.1$; Figure 9b). High MWIR transparency was maintained in these CHIPs materials, as confirmed from MWIR thermal imaging through melt processed windows of both USAF targets and a human arm (Figure 9c−f). The Mecerreyes group utilized a similar inverse vulcanization approach to prepare S-Se terpolymers as cathode materials for Li-sulfur batteries and found the inclusion of selenium improved battery performance under high cycle rates.96

Synthetic access to ultrahigh refractive index CHIPs from S-Se terpolymers allowed for the fabrication of highly reflective, wholly polymeric 1D photonic crystals (1D PCs) from solution processing. 1D PCs are alternating layers of low and high refractive index material and are used in a variety of applications including sensors⁹⁷ and lasing from all-polymer microcavities. 98 The photonic band gap (PBG) of 1D PCs can be tuned by adjusting the thickness of each layer, while the magnitude of the resulting reflection is proportional to the difference in refractive index between the layers. Given these considerations, metal oxides, chalcogens, and semiconductors are often used in conjunction to fabricate 1D PCs. Using these materials, a large refractive index contrast (Δn) between layers is easily achieved, and precise control over layer thickness is accomplished using vapor deposition methods. Wholly polymeric 1D PCs have also been investigated that are

amenable to large-scale solution and melt processing and are generally more flexible. Toward this end, poly(S-r-Se-r-DIB) and cellulose acetate were used to generate a large difference in refractive index ($\Delta n = 0.5$) in a wholly polymeric 1D PC assembled by spin-coating with 20–30 layers. This process afforded 1D PCs with high reflectivity (>90%) and a tunable bandgap across the SWIR.

Long-wave infrared imaging with CHIPs: Long-wave infrared (LWIR) thermal imaging $(7-14 \mu m)$ offers important advantages for high-resolution imaging in near or complete darkness, which has widely been exploited in defense applications. However, given the inherently lower cost of LWIR imaging systems, the development of low-cost plastic optics for consumer applications is anticipated to lower the overall cost of LWIR cameras and enable entry into the consumer markets mentioned previously. The-state-of-the-art transmissive materials used for LWIR imaging are largely limited to germanium (Ge) or chalcogenide glasses (ChGs) for freestanding optical elements. The development of low-cost and processable transmissive plastics would offer numerous manufacturing and processing advantages, but generally suffer from low transparency and a low refractive index in the LWIR spectrum. A major challenge in the design of LWIR transparent organic materials is the fact that nearly all organic molecules and polymers absorb in this spectral window that lies within the "IR fingerprint region".

A notable first demonstration of making polymers with improved LWIR transparency was reported by Boyd et al. in 2019, where a CHIPs material was synthesized using tetravinyl tin comonomer as the organic cross-linker (Figure 10). This material exhibited the anticipated MWIR transparency and high refractive index (n < 2.0) as a consequence of the chalcogenide and tin units in the final copolymer. Furthermore, the authors demonstrate melt processing of freestanding films of at least 1 mm in thickness for a demonstration of LWIR imaging of a metallic soldering iron at an elevated temperature. This exciting discovery has since prompted very recent efforts to both improve LWIR transparency and thermomechanical properties of the resulting polymeric transmissive materials for optical element fabrication.

An intriguing report on the synthesis of new CHIPs materials was reported by Lee et al. in 2019 that described

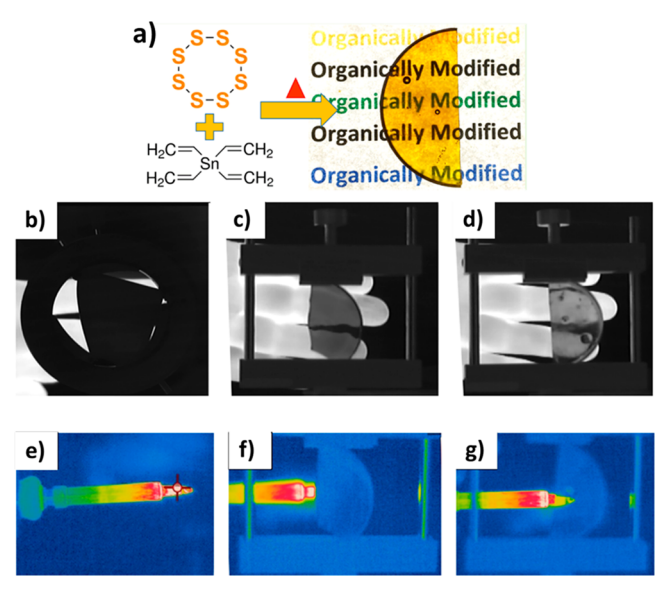
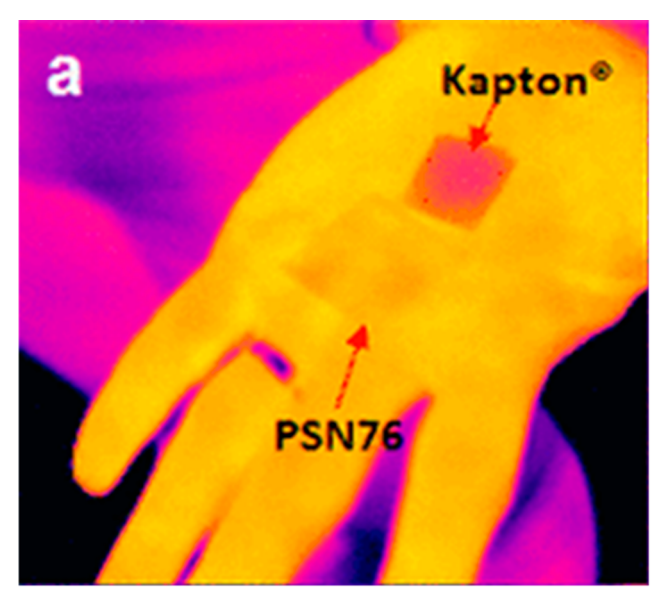


Figure 10. (a) Synthesis of poly(S-r-TVSn); MWIR (3–5 μ m) images of human fingers viewed (b) through 1.50 mm thick PMMA; (c) through 1.63 mm thick poly(S-r-DIB), and (d) through 1.65 mm thick poly(S-r-TVSn); LWIR (7.5–14 μ m) images of a hot soldering iron viewed (e) in open air, (f) through 1.63 mm thick poly(S-r-DIB), and (g) through 1.65 mm thick poly(S-r-TVSn). Adapted with permission from ref 100. Copyright 2019 American Chemical Society.

the use of active di-iodobenzene organic comomomers for inverse vulcanization with sulfur to form polyphenylpolysulfide-based materials. 101 This demonstration leveraged the development of salt-free methods for the preparation of polyphenylsulfide using aryl iodide-based comonomers. 102,103 The authors further reported on the use of freestanding films of these polymers prepared by melt processing (film thickness $\sim 200 \ \mu \text{m}$) for LWIR imaging (Figure 11). While sufficient LWIR transparency was observed when imaged through 200 μ m films of these CHIPs materials, the use of thin films is a technical concern, since even conventional polymers, such as polystyrene or PMMA, can exhibit some LWIR transparency at these thicknesses. Hence, for bulk IR optical elements, characterization of thin film samples is not sufficient for evaluation of these polymers as a LWIR transmissive material. It is therefore important to demonstrate processing and fabrication methods sufficient to prepare thick enough (~1 mm) optical elements to enable both rigorous IR spectroscopic and thermal imaging evaluation. A recent report on thin films of high RI polyimides that have a high content of aromatic units (that are strongly LWIR absorbing) 104 is also illustrative of the potential for erroneous claims and warrants a need for clear metrics for optical characterization of LWIR transmissive materials. These technical concerns regarding IR imaging in no way detracts from the elegance of the polymer chemistry of this report, but simply points to the challenges of associated with developing LWIR polymeric materials.

Infrared fingerprint engineering: Numerous fundamental chemistry challenges arise in true molecular design concepts for creating organic comonomers and polymers with LWIR transparency. As previously discussed, the chemical design principle for improving MWIR transparency from 3 to 5 μ m is the elimination or minimization of C–H, O–H, and N–H in the transmissive polymeric material. However, rational molecular design of LWIR transparency is profoundly more complex due to the numerous fundamental and non-



Poly(phenylene polysulfide) Networks from Elemental Sulfur & p-Diidobenzene

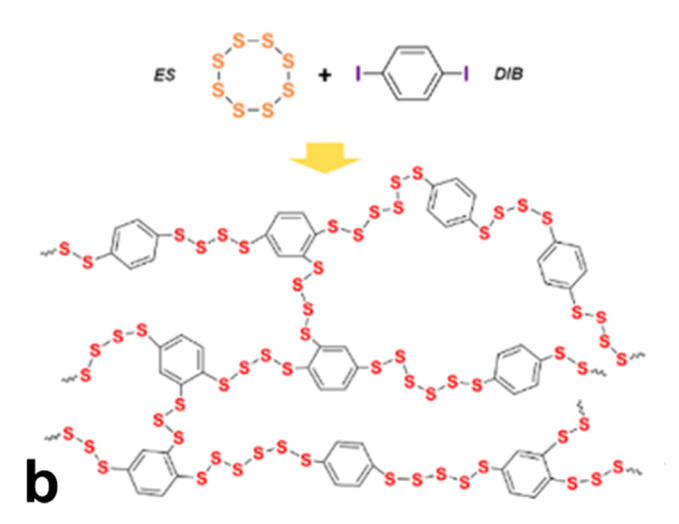


Figure 11. (a) IR thermal image of PSN76 and Kapton polyimide films on the hand of a human subject. Thermal images of a male subject captured with a long-IR $(7.5-13 \, \mu \text{m})$ camera; (b) Synthesis of poly(phenylene polysulfide) networks (PSNs) from elemental sulfur and p-di-iodobenzene. Reproduced with permission from ref 101. Copyright 2019 American Chemical Society.

fundamental bond vibrations observed in organic materials and is a new technical area of research with tremendous technological potential that we describe as "IR Fingerprint Engineering". In order to accelerate materials design and synthesis, Pyun and co-workers at the University of Arizona exploited the use of computational chemistry, specifically, density functional theory (DFT) calculations to simulate the IR spectra of candidate comonomers and CHIPs materials for improved LWIR transparency. 106 Using computational simulations, the design of a dimeric monomer from 2,5norbornadiene (NBD2) was developed that exhibited low LWIR absorbance in these calculations (Figure 12c), while still retaining reactive groups for polymerization with sulfur. Copolymerization of these comonomers were observed to afford amorphous, yellow glassy, crosslinked networks of poly(S-r-NBD2). These thermosets were observed to possess

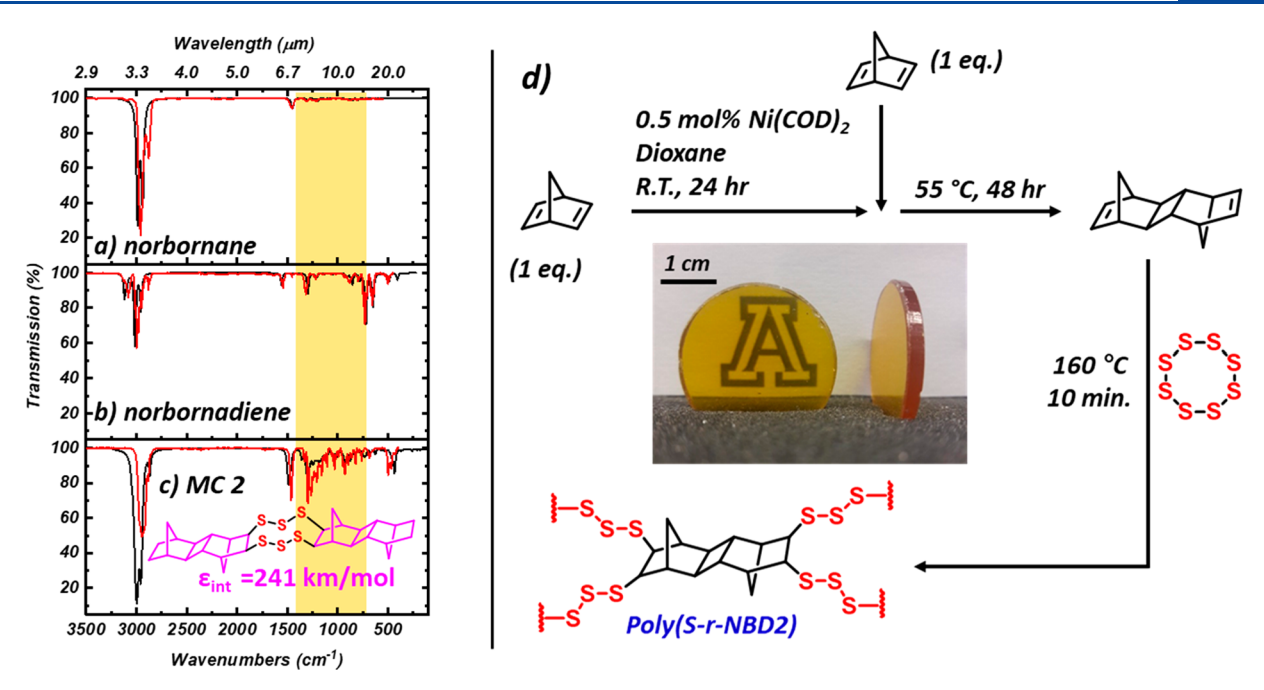


Figure 12. Comparison of DFT calculated FTIR spectra for equal concentrations of (a) norbornane, (b) 2,5-norbornadiene, and (c) MC 2 (black lines). Red line indicates experimental gas-phase spectra of (a) norbornane, 105 (b) 2,5-norbornadiene, 105 and (c) experimental FTIR spectra of poly(S_{70} -r-NBD2 $_{30}$). (d) Synthetic scheme for synthesis of NBD2 via the nickel catalyzed [2 + 2] cycloaddition of 2,5-norbornadiene and the inverse vulcanization of NBD2 with elemental sulfur; image shown consists of two 2.3 mm thick diamond polished windows of poly(S_{50} -r-NBD2 $_{50}$), where both originated from an originally 3.4 mm thick cast sample. Adapted with permission from ref 106. Copyright 2019 John Wiley & Sons. Logo courtesy of the University of Arizona.

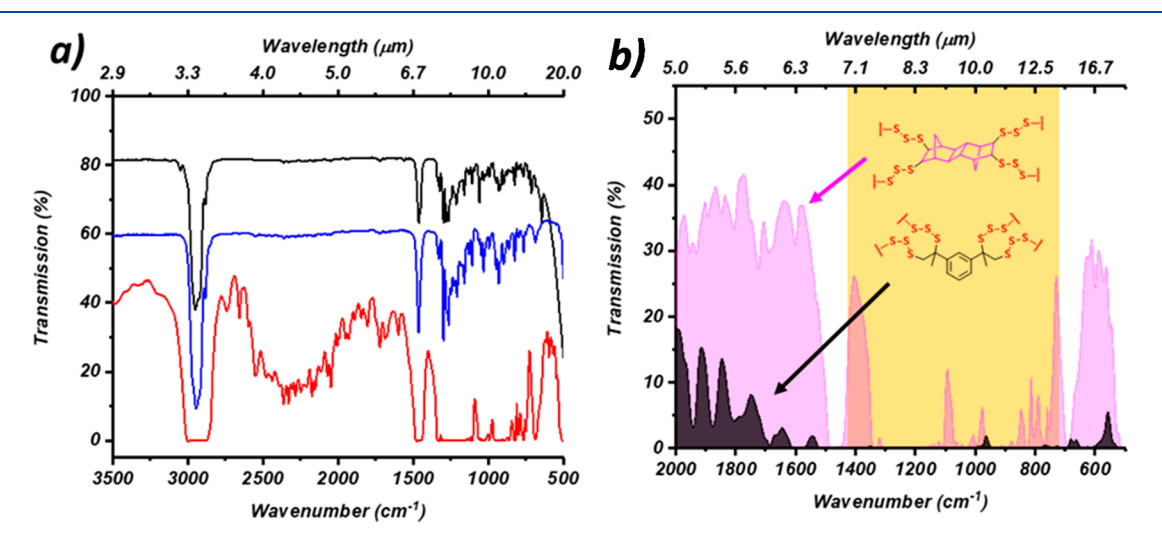


Figure 13. (a) Stacked FTIR spectra of poly(S_{70} -r-NBD2 $_{30}$) at varying thicknesses from \sim 5–30 μ m on a NaCl plate (black line), 60 μ m (blue line) and 1 mm free-standing films (red line); (b) expanded region of the midlong wave IR spectrum of 1 mm thick films of poly(S_{70} -r-NBD2 $_{30}$) and poly(S_{70} -r-DIB $_{30}$) with the 7–14 μ m regime shaded. Adapted with permission from ref 106. Copyright 2019 John Wiley & Sons.

an enhanced glass transition ($T_{\rm g} \sim 100~{\rm ^{\circ}C}$) and thermal stability with thermal properties approximating those for PMMA, which is one of the optical industry standards for polymeric optical elements. The thermomechanical features of this new CHIPs thermoset offered significant melt processing advantages for the fabrication of thicker optical elements (1–3 mm in thickness), namely, windows, which were amenable for the first time for CHIPs materials to diamond polishing to fabricate high quality optical elements (Figure 12d).

A challenging but critical aspect of the optical characterization of these materials were IR spectroscopic and thermal imaging experiments to enable comparative evaluation of

polymers for LWIR transmissive materials. IR spectroscopy is a central characterization tool determining windows of transparency and for quantifying transmittance for thicker polymer films. While thin film samples on salt plates are sufficient to qualitatively access IR absorptions for functional groups, IR spectroscopic analysis of thicker free-standing films are required for assessment of overall IR transparency for free-standing optical elements (Figure 13a). For evaluation of LWIR transparency for different candidate materials, the development of robust processing protocols for preparing polymer films of identical film thicknesses were required to quantify differences in IR transmittance, since even small

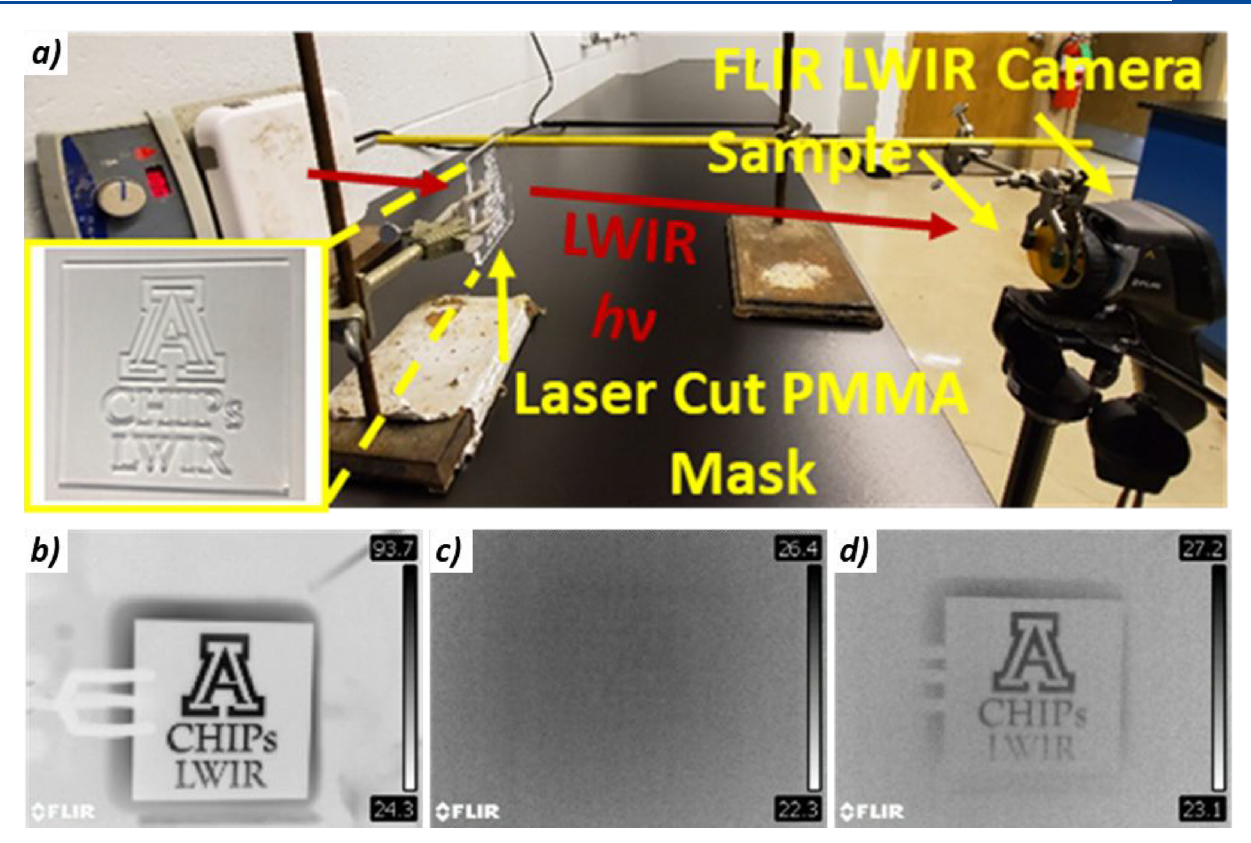


Figure 14. (a) Digital image of LWIR imaging set up and LWIR images taken with a FLIR LWIR camera operating in the 7.5–13 μ m regime in "black hot" mode with inset of patterned PMMA sheet (12 × 12 cm) used as mask for LWIR imaging; (b) no window in front of the camera; (c) through a 1.3 \pm 0.15 mm thick poly(S_{70} -r-DIB $_{30}$) window; and (d) through a 1.3 \pm 0.12 mm thick poly(S_{70} -r-NBD2 $_{30}$) window. Reproduced with permission from ref 106. Copyright 2019 John Wiley & Sons. Logo courtesy of the University of Arizona.

variations in film thickness can lead to misleading interpretation of LWIR transparency. Comparative studies of poly(S-r-DIB) versus poly(S-r-NBD2) films using IR spectroscopy confirmed that the C=C bonds on the aromatic groups in poly(S-r-DIB) strongly absorbed in the LWIR region. For these studies, 1 mm thick windows of poly(S-r-DIB) versus poly(S-r-NBD2) of the same copolymer composition (70 wt % S; 30-wt % organic comonomer) were analyzed by IR spectroscopy, which confirmed almost complete opacity for poly(S-r-DIB) samples from 7 to 14 μ m, while poly(S-r-NBD2) exhibited numerous windows of LWIR transmittance at 7–7.5, 9.1–9.4, 10.2–10.5, and 13.4–14.6 μ m (Figure 13b).

LWIR thermal imaging experiments with poly(S-r-NBD2) thermoset windows were conducted as a final assessment of optical transparency. Windows or films with a minimum thickness of 1 mm were required to conduct meaningful LWIR measurements, as even conventional vinyl and aromatic-based polymers at thicknesses below 500 μ m commonly display some LWIR transparency, but would not be considered viable transmissive materials for free-standing optical elements. This criterion also indirectly requires the development of viable polymer processing and postprocessing steps to enable creation of high quality optical elements. To enable a systematic variation of imaging conditions, a straightforward system consisting of a LWIR camera and a temperature controlled hot plate (as a blackbody radiator and IR source for imaging) was assembled (Figure 14). To facilitate image processing, a pattern was cut into a 4 mm thick PMMA sheet using a CO₂ laser (Figure 14a), followed by placing a CHIPs window of at least 1 mm thickness in front of the LWIR

camera. Imaging control experiments of the patterned PMMA sheet without a CHIPs window revealed high resolution imaging at $T=100\,^{\circ}\mathrm{C}$ (Figure 14b). Complete loss of LWIR imaging was observed for experiments conducted with poly(S-r-DIB) windows due to strong absorbance from aromatic moieties in the copolymer. (Figure 14c). However, when windows of similar thickness prepared from poly(S-r-NBD2) were used, LWIR imaging was restored as noted by clear resolution of the patterned PMMA sheet (Figure 14d).

Perspective and future outlook: As discussed in this Review, the development of high refractive index polymers for IR thermal imaging and optics is an exciting new direction in polymer science. The pioneering findings discussed in this report point to the ability of the organic comonomer design to profoundly affect bulk thermomechanical and optical properties, which reveals the potential of polymer chemistry to create new and improved materials for this application. In addition to copolymer design and synthesis, the development of new and diverse polymerization methods using elemental sulfur is an important emerging area that warrants further exploration. From a materials standpoint, the thermomechanical properties of high refractive index polymers from elemental sulfur need to be improved to survive processing conditions and device integration into IR imaging systems. These materials properties will remain technically challenging since functional groups that enhance optical properties (e.g., RI and IR transparency) often compromise thermomechanical features of the (co)polymeric product. The use of computational chemistry and machine learning tools also points to a new direction to accelerate new materials discovery. Hence, it is clear that there is a strong

need for new synthetic polymer chemistry methodology to meet these difficult barriers in this nascent field. We would also like to point out the importance of standardizing analyses and performance metrics for these materials as characterization of CHIPs can present unique challenges. A critical aspect that has been routinely overlooked is the determination of refractive indices for CHIPs materials at wavelengths beyond the SWIR. The noted absorptions of CHIPs materials at or near the midand long wavelengths of interest will have an effect on the refractive indices of these materials at those wavelengths, and knowledge of those values is critical for designing optical elements. Prism coupling is an excellent method for obtaining absolute values of the refractive index in the visible and SWIR regions, but light sources and prisms appropriate for longer wavelengths are generally not available. Spectroscopic ellipsometry measurements can be performed throughout the infrared region, and we recommend coupling spectroscopic ellipsometry, which provides excellent relative knowledge of the refractive index as a function of wavelength, with prism coupling measurements in the visible and SWIR to provide absolute calibration. Another crucial measurement in need of standardization concerns the thickness of CHIPs windows/ lenses used to evaluate IR transparency. As stated before, transparency of thin films (~microns in thickness) can be unintentionally misleading, whereas at least 1 mm thick windows provide a demonstration of transparency more suited toward end-use applications. Other optical properties relevant to the design of optical elements are the thermo-optic coefficient (dn/dt) and the stress optic coefficient. The methods used to obtain these values require expertise and measurement platforms not necessarily available to all research groups, but do need to be addressed as the field of IR plastics advances, especially given that these effects are known to be more dramatic for polymer-based systems compared to inorganic materials. Lastly, with regard to (thermo)mechanical characterization, we suggest all standard measurements and analyses be carried out where possible as they would for any other new polymeric material. Paired with the exciting advancements in chemistry related to IR polymers, these standardized analyses will serve to define the new role IR plastics will be able to play in infrared imaging.

AUTHOR INFORMATION

Corresponding Authors

Robert A. Norwood — Wyant College of Optical Sciences, The University of Arizona, Tucson, Arizona 85721, United States; Email: rnorwood@optics.arizona.edu

Jeffrey Pyun — Department of Chemistry and Biochemistry, The University of Arizona, Tucson, Arizona 85721, United States; orcid.org/0000-0002-1288-8989; Email: jpyun@email.arizona.edu

Authors

Tristan S. Kleine — Department of Chemistry and Biochemistry, The University of Arizona, Tucson, Arizona 85721, United States

Richard S. Glass – Department of Chemistry and Biochemistry, The University of Arizona, Tucson, Arizona 85721, United States

Dennis L. Lichtenberger — Department of Chemistry and Biochemistry, The University of Arizona, Tucson, Arizona 85721, United States; orcid.org/0000-0002-9271-0311

Michael E. Mackay — Department of Materials Science & Engineering, Department of Chemical Engineering, University of Delaware, Newark, Delaware 19711, United States;

orcid.org/0000-0003-1652-9139

Kookheon Char — School of Chemical and Biological Engineering, Seoul 151-744, Republic of Korea; ⊚ orcid.org/ 0000-0002-7938-8022

Complete contact information is available at: https://pubs.acs.org/10.1021/acsmacrolett.9b00948

Notes

The authors declare no competing financial interest.

ACKNOWLEDGMENTS

We acknowledge the NSF (DMR-1607971, CHE-1807395), the College of Science from the University of Arizona, TRIF/University of Arizona, the AFOSR Phase II STTR Contract (FA9550-17-C-005) and MOBASE for support of this work.

REFERENCES

- (1) Herschel, W. XIII. Investigation of the Powers of the Prismatic Colours to Heat and Illuminate Objects; with Remarks, That Prove the Different Refrangibility of Radiant Heat. To Which Is Added, an Inquiry into the Method of Viewing the Sun Advantageously, with Telesco. *Philosophical Trans* **1800**, *90*, 255–283.
- (2) Planck, M. On the Law of Distribution of Energy in the Normal Spectrum. *Ann. Phys.* **1901**, *309*, 553.
- (3) Vollmer, M.; Möllmann, K.-P. *Infrared Thermal Imaging*, 2nd ed.; Wiley: Weinheim, Germany, 2017.
- (4) Griebel, J. J.; Glass, R. S.; Char, K.; Pyun, J. Polymerizations with Elemental Sulfur: A Novel Route to High Sulfur Content Polymers for Sustainability, Energy and Defense. *Prog. Polym. Sci.* **2016**, *58*, 90–125.
- (5) Zhang, Y.; Glass, R. S.; Char, K.; Pyun, J. Recent Advances in the Polymerization of Elemental Sulphur, Inverse Vulcanization and Methods to Obtain Functional Chalcogenide Hybrid Inorganic/Organic Polymers (CHIPs). *Polym. Chem.* **2019**, *10* (30), 4078–4105.
- (6) Lim, J.; Pyun, J.; Char, K. Recent Approaches for the Direct Use of Elemental Sulfur in the Synthesis and Processing of Advanced Materials. *Angew. Chem., Int. Ed.* **2015**, *54* (11), 3249–3258.
- (7) Hansen, M. P.; Malchow, D. S. Overview of SWIR Detectors, Cameras, and Applications. *Thermosense XXX: Proceedings of SPIE*, Orlando, FL, March, 2008, Society of Photo Optical, 2008, 6930I, 1–11.
- (8) Dwivedi, R. S. An Introduction to Remote Sensing. Remote Sensing of Soils; Springer: Berlin, Heidelberg, 2017; pp 1-47.
- (9) Brennan, K. F.; Haralson, J., II Invited Review: Superlattice and Multiquantum Well Avalanche Photodetectors: Physics, Concepts and Performance. *Superlattices Microstruct.* **2000**, 28 (2), 77–104.
- (10) Kastberger, G.; Stachl, R. Infrared Imaging Technology and Biological Applications. *Behav. Res. Methods Instrum. Comput.* **2003**, 35 (3), 429–439.
- (11) Mambou, S. J.; Maresova, P.; Krejcar, O.; Selamat, A.; Kuca, K. Breast Cancer Detection Using Infrared Thermal Imaging and a Deep Learning Model. *Sensors* **2018**, *18* (9), 2799.
- (12) Jones, B. F. A Reappraisal of the Use of Infrared Thermal Image Analysis in Medicine. *IEEE Trans. Med. Imag.* **1998**, *17* (6), 1019–1027.
- (13) Ring, E. F. J.; Ammer, K. Infrared Thermal Imaging in Medicine. *Physiol. Meas.* **2012**, *33* (3), R33–R46.
- (14) Rakha, T.; Gorodetsky, A. Review of Unmanned Aerial System (UAS) Applications in the Built Environment: Towards Automated Building Inspection Procedures Using Drones. *Autom. Constr.* **2018**, 93, 252–264.

- (15) Balaras, C. A.; Argiriou, A. A. Infrared Thermography for Building Diagnostics. *Energy Build* **2002**, *34* (2), 171–183.
- (16) Bagavathiappan, S.; Lahiri, B. B.; Saravanan, T.; Philip, J.; Jayakumar, T. Infrared Thermography for Condition Monitoring A Review. *Infrared Phys. Technol.* **2013**, *60*, 35–55.
- (17) Huda, A. S. N.; Taib, S. Application of Infrared Thermography for Predictive/Preventive Maintenance of Thermal Defect in Electrical Equipment. *Appl. Therm. Eng.* **2013**, *61* (2), 220–227.
- (18) Jadin, M. S.; Taib, S. Recent Progress in Diagnosing the Reliability of Electrical Equipment by Using Infrared Thermography. *Infrared Phys. Technol.* **2012**, 55 (4), 236–245.
- (19) Usamentiaga, R.; Venegas, P.; Guerediaga, J.; Vega, L.; Molleda, J.; Bulnes, G. F. Infrared Thermography for Temperature Measurement and Non-Destructive Testing. *Sensors* **2014**, *14* (7), 12305–12348
- (20) Hagen, N. A.; Kudenov, M. W. Review of Snapshot Spectral Imaging Technologies. *Opt. Eng.* **2013**, 52 (9), 1–23.
- (21) Morales-Rodríguez, M. E.; Senesac, L. R.; Thundat, T.; Rafailov, M. K.; Datskos, P. G. Standoff Imaging of Chemicals Using IR Spectroscopy. *Micro- and Nanotechnology Sensors, Systems, and Applications III*; Proceedings of SPIE, Orlando, 2011, 80312D, 1–8.
- (22) Bernacki, B. E.; Phillips, M. C. Standoff Hyperspectral Imaging of Explosives Residues Using Broadly Tunable External Cavity Quantum Cascade Laser Illumination. *Chemical, Biological, Radiological, Nuclear and Explosives (CBRNE) Sensing XI*; Proceedings of SPIE, Orlando, 2010, 76650I, 1–10.
- (23) Blake, T. A.; Kelly, J. F.; Gallagher, N. B.; Gassman, P. L.; Johnson, T. J. Passive Standoff Detection of RDX Residues on Metal Surfaces via Infrared Hyperspectral Imaging. *Anal. Bioanal. Chem.* **2009**, 395 (2), 337–348.
- (24) Fuchs, F.; Hugger, S.; Jarvis, J.; Blattmann, V.; Kinzer, M.; Yang, Q. K.; Ostendorf, R.; Bronner, W.; Driad, R.; Aidam, R.; Wagner, J. Infrared Hyperspectral Standoff Detection of Explosives. *Chemical, Biological, Radiological, Nuclear and Explosives (CBRNE) Sensing XIV*; Proceedings of SPIE, Orlando, 2013, 87100I, 1–8.
- (25) Van der Meer, F. D.; Van der Werff, H. M. A.; Van Ruitenbeek, F. J. A.; Hecker, C. A.; Bakker, W. H.; Noomen, M. F.; Van der Meijde, M.; Carranza, E. J. M.; de Smeth, J. B.; Woldai, T. Multi- and Hyperspectral Geologic Remote Sensing: A Review. *ITC J.* **2012**, *14* (1), 112–128.
- (26) Christensen, P. R.; Jakosky, B. M.; Kieffer, H. H.; Malin, M. C.; McSween, H. Y.; Nealson, K.; Mehall, G. L.; Silverman, S. H.; Ferry, S.; Caplinger, M.; Ravine, M. The Thermal Emission Imaging System (THEMIS) for the Mars 2001 Odyssey Mission. In 2001 Mars Odyssey; Russell, C. T., Ed.; Springer: Dordrecht, 2004; pp 85–130.
- (27) Rogalski, A. History of Infrared Detectors. Opto-Electron. Rev. 2012, 20 (3), 279-308.
- (28) Kruse, P. W. The Emergence of $Hg_{1-x}Cd_xTe$ as a Modern Infrared Sensitive Material. In *Semiconductors and Semimetals*; Willardson, R. K., Beer, A. C., Eds.; Academic Press: New York, NY, 1981; Vol. 18, pp 1–20.
- (29) Karim, A.; Andersson, J. Y. Infrared Detectors: Advances, Challenges and New Technologies. *IOP Conf. Ser.: Mater. Sci. Eng.* **2013**, *51*, 012001.
- (30) Narlis, E. O. Comparative Performance Analysis of the MWIR and LWIR Focal Plane Array Starring Imaging Infrared Systems. *Int. J. Infrared Millimeter Waves* **2002**, 23 (3), 393–408.
- (31) Coffey, V. C. Seeing in the Dark: Defense Applications of IR Imaging. Opt. Photonics News 2011, 22 (4), 26–31.
- (32) Rogalski, A. Infrared Detectors for the Future. *Acta Phys. Pol., A* **2009**, *116*, 389.
- (33) Wood, R. A.; Han, C. J.; Kruse, P. W. Integrated Uncooled Infrared Detector Imaging Arrays. Proceedings of Technical Digest IEEE Solid-State Sensor and Actuator Workshop, Hilton Head Island, 1992, IEEE, 1992, pp 132–135.
- (34) Wang, B.; Lai, J.; Li, H.; Hu, H.; Chen, S. Nanostructured Vanadium Oxide Thin Film with High TCR at Room Temperature for Microbolometer. *Infrared Phys. Technol.* **2013**, *57*, 8–13.

- (35) Codreanu, I.; Gonzalez, F. J.; Boreman, G. D. Detection Mechanisms in Microstrip Dipole Antenna-Coupled Infrared Detectors. *Infrared Phys. Technol.* **2003**, 44 (3), 155–163.
- (36) Rogalski, A. Recent Progress in Infrared Detector Technologies. *Infrared Phys. Technol.* **2011**, *54* (3), 136–154.
- (37) Choi, Y.; Kim, N.; Hwang, S.; Park, K.; Yoon, J. S.; An, K.; Kweon, I. S. KAIST Multi-Spectral Day/Night Data Set for Autonomous and Assisted Driving. *IEEE Trans. Intell. Transp. Syst.* **2018**, *19* (3), 934–948.
- (38) Zhang, X. H.; Guimond, Y.; Bellec, Y. Production of Complex Chalcogenide Glass Optics by Molding for Thermal Imaging. *J. Non-Cryst. Solids* **2003**, 326-327, 519–523.
- (39) Rankin, A.; Huertas, A.; Matthies, L.; Bajracharya, M.; Assad, C.; Brennan, S.; Bellutta, P.; Sherwin, G. W. Unmanned Ground Vehicle Perception Using Thermal Infrared Cameras. *Unmanned Systems and Technology XIII*; Proceedings of SPIE, Orlando, 2011, 804503, 1–26.
- (40) Zhang, X.; Bureau, B.; Lucas, P.; Boussard-Pledel, C.; Lucas, J. Glasses for Seeing Beyond Visible. *Chem. Eur. J.* **2008**, *14* (2), 432–442.
- (41) Lucas, P.; Coleman, G. J.; Jiang, S.; Luo, T.; Yang, Z. Chalcogenide Glass Fibers: Optical Window Tailoring and Suitability for Bio-Chemical Sensing. *Opt. Mater.* **2015**, *47*, 530–536.
- (42) Depuydt, B.; Theuwis, A.; Romandic, I. Germanium: From the First Application of Czochralski Crystal Growth to Large Diameter Dislocation-Free Wafers. *Mater. Sci. Semicond. Process.* **2006**, 9 (4), 437–443.
- (43) Kulakova, N. A.; Nasyrov, A. R.; Nesmelova, I. M. Current Trends in Creating Optical Systems for the IR Region. *J. Opt. Technol.* **2010**, 77 (5), 324–330.
- (44) Cha, D. H.; Kim, H.-J.; Hwang, Y.; Jeong, J. C.; Kim, J.-H. Fabrication of Molded Chalcogenide-Glass Lens for Thermal Imaging Applications. *Appl. Opt.* **2012**, *51* (23), 5649–5656.
- (45) Eggleton, B. J.; Luther-Davies, B.; Richardson, K. Chalcogenide Photonics. *Nat. Photonics* **2011**, 5 (3), 141–148.
- (46) Kreidl, N. J.; Ratzenboeck, W. Structure of Chalcogenide Glasses. In *Recent Advances in Science and Technology of Materials*; Bishay, A., Ed.; Springer: Boston, MA, 1974; pp 153–170.
- (47) Hilton, A. R. Optical Properties of Chalcogenide Glasses. J. Non-Cryst. Solids 1970, 2, 28–39.
- (48) Borisova, Z. U. Glassy Semiconductors; Springer: Boston, MA, 1981.
- (49) Leadbetter, A. J.; Apling, A. J. Diffraction Studies of Glass Structure: (V). The Structure of Some Arsenic Chalcogenide Glasses. *J. Non-Cryst. Solids* **1974**, *15* (2), 250–268.
- (50) Musgraves, J. D.; Danto, S.; Richardson, K. Thermal Properties of Chalcogenide Glasses. In *Chalcogenide Glasses: Preparation, Properties and Applications*; Adam, J.-L., Zhang, X., Eds.; Woodhead Publishing, 2014; pp 82–112.
- (51) Mineral Commodities Summary; U.S. Geological Survey, 2019, DOI: 10.3133/70202434.
- (52) Churbanov, M. F. Recent Advances in Preparation of High-Purity Chalcogenide Glasses in the USSR. *J. Non-Cryst. Solids* **1992**, 140, 324–330.
- (53) Bowden, B. F.; Harrington, J. A. Fabrication and Characterization of Chalcogenide Glass for Hollow Bragg Fibers. *Appl. Opt.* **2009**, *48* (16), 3050–3054.
- (54) Sanghera, J. S.; Aggarwal, I. D. Active and Passive Chalcogenide Glass Optical Fibers for IR Applications: A Review. *J. Non-Cryst. Solids* 1999, 256–257, 6–16.
- (55) Zha, Y.; Waldmann, M.; Arnold, C. B. A Review on Solution Processing of Chalcogenide Glasses for Optical Components. *Opt. Mater. Express* **2013**, 3 (9), 1259–1272.
- (56) Slang, S.; Palka, K.; Janicek, P.; Grinco, M.; Vlcek, M. Solution Processed As30Se70 Chalcogenide Glass Thin Films with Specular Optical Quality: Multi-Component Solvent Approach. *Opt. Mater. Express* **2018**, 8 (4), 948–959.
- (57) Chern, G. C.; Lauks, I. Spin-coated Amorphous Chalcogenide Films. J. Appl. Phys. 1982, 53 (10), 6979–6982.

- (58) Chern, G. C.; Lauks, I. Spin Coated Amorphous Chalcogenide Films: Structural Characterization. *J. Appl. Phys.* **1983**, *54* (5), 2701–2705
- (59) Tsay, C.; Mujagić, E.; Madsen, C. K.; Gmachl, C. F.; Arnold, C. B. Mid-Infrared Characterization of Solution-Processed As₂S₃ Chalcogenide Glass Waveguides. *Opt. Express* **2010**, *18* (15), 15523–15530.
- (60) Brette, N. A.; Klocek, P. Engineered Polymeric IR-Transparent Protective Coatings. *Windows and Dome Technologies and Materials IV*; Proceedings of SPIE, San Diego, 1994, 2286, 325–334.
- (61) Claytor, N.; Claytor, R. Polymer Imaging Optics for the Thermal Infrared. *Infrared Technology and Applications XXX*; Proceedings of SPIE, Orlando, 2004, 107–113.
- (62) Chung, W. J.; Griebel, J. J.; Kim, E. T.; Yoon, H.; Simmonds, A. G.; Ji, H. J.; Dirlam, P. T.; Glass, R. S.; Wie, J. J.; Nguyen, N. A.; Guralnick, B. W.; Park, J.; Somogyi, Á.; Theato, P.; Mackay, M. E.; Sung, Y.-E.; Char, K.; Pyun, J. The Use of Elemental Sulfur as an Alternative Feedstock for Polymeric Materials. *Nat. Chem.* **2013**, *5* (6), 518–524.
- (63) Martin, T. R.; Mazzio, K. A.; Hillhouse, H. W.; Luscombe, C. K. Sulfur Copolymer for the Direct Synthesis of Ligand-Free CdS Nanoparticles. *Chem. Commun.* **2015**, *51* (56), 11244–11247.
- (64) Gomez, I.; Mecerreyes, D.; Blazquez, J. A.; Leonet, O.; Ben Youcef, H.; Li, C.; Gómez-Cámer, J. L.; Bondarchuk, O.; Rodriguez-Martinez, L. Inverse Vulcanization of Sulfur with Divinylbenzene: Stable and Easy Processable Cathode Material for Lithium-Sulfur Batteries. *J. Power Sources* **2016**, 329, 72–78.
- (65) Dirlam, P. T.; Simmonds, A. G.; Shallcross, R. C.; Arrington, K. J.; Chung, W. J.; Griebel, J. J.; Hill, L. J.; Glass, R. S.; Char, K.; Pyun, J. Improving the Charge Conductance of Elemental Sulfur via Tandem Inverse Vulcanization and Electropolymerization. *ACS Macro Lett.* **2015**, *4* (1), 111–114.
- (66) Gomez, I.; De Anastro, A. F.; Leonet, O.; Blazquez, J. A.; Grande, H.-J.; Pyun, J.; Mecerreyes, D. Sulfur Polymers Meet Poly(Ionic Liquid)s: Bringing New Properties to Both Polymer Families. *Macromol. Rapid Commun.* **2018**, 39 (21), 1800529.
- (67) Zhang, Y.; Griebel, J. J.; Dirlam, P. T.; Nguyen, N. A.; Glass, R. S.; Mackay, M. E.; Char, K.; Pyun, J. Inverse Vulcanization of Elemental Sulfur and Styrene for Polymeric Cathodes in Li-S Batteries. J. Polym. Sci., Part A: Polym. Chem. 2017, 55 (1), 107–116. (68) Wu, X.; Smith, J. A.; Petcher, S.; Zhang, B.; Parker, D. J.; Griffin, J. M.; Hasell, T. Catalytic Inverse Vulcanization. Nat. Commun. 2019, 10 (1), 647.
- (69) Yan, L.; Han, D.; Xiao, M.; Ren, S.; Li, Y.; Wang, S.; Meng, Y. Instantaneous Carbonization of an Acetylenic Polymer into Highly Conductive Graphene-like Carbon and Its Application in Lithium—Sulfur Batteries. J. Mater. Chem. A 2017, 5 (15), 7015—7025.
- (70) Dirlam, P. T.; Simmonds, A. G.; Kleine, T. S.; Nguyen, N. A.; Anderson, L. E.; Klever, A. O.; Florian, A.; Costanzo, P. J.; Theato, P.; Mackay, M. E.; Glass, R. S.; Char, K.; Pyun, J. Inverse Vulcanization of Elemental Sulfur with 1,4-Diphenylbutadiyne for Cathode Materials in Li-S Batteries. *RSC Adv.* **2015**, *5* (31), 24718–24722.
- (71) Crockett, M. P.; Evans, A. M.; Worthington, M. J. H.; Albuquerque, I. S.; Slattery, A. D.; Gibson, C. T.; Campbell, J. A.; Lewis, D. A.; Bernardes, G. J. L.; Chalker, J. M. Sulfur-Limonene Polysulfide: A Material Synthesized Entirely from Industrial By-Products and Its Use in Removing Toxic Metals from Water and Soil. *Angew. Chem., Int. Ed.* **2016**, *55* (5), 1714–1718.
- (72) Parker, D. J.; Jones, H. A.; Petcher, S.; Cervini, L.; Griffin, J. M.; Akhtar, R.; Hasell, T. Low Cost and Renewable Sulfur-Polymers by Inverse Vulcanisation, and Their Potential for Mercury Capture. *J. Mater. Chem. A* **2017**, *5* (23), 11682–11692.
- (73) Lundquist, N. A.; Worthington, M. J. H.; Adamson, N.; Gibson, C. T.; Johnston, M. R.; Ellis, A. V.; Chalker, J. M. Polysulfides Made from Re-Purposed Waste Are Sustainable Materials for Removing Iron from Water. *RSC Adv.* **2018**, *8* (3), 1232–1236.
- (74) Worthington, M. J. H.; Shearer, C. J.; Esdaile, L. J.; Campbell, J. A.; Gibson, C. T.; Legg, S. K.; Yin, Y.; Lundquist, N. A.; Gascooke, J. R.; Albuquerque, I. S.; Shapter, J. G.; Andersson, G. G.; Lewis, D. A.;

- Bernardes, G. J. L.; Chalker, J. M. Sustainable Polysulfides for Oil Spill Remediation: Repurposing Industrial Waste for Environmental Benefit. *Adv. Sustainable Syst.* **2018**, 2 (6), 1800024.
- (75) Worthington, M. J. H.; Kucera, R. L.; Albuquerque, I. S.; Gibson, C. T.; Sibley, A.; Slattery, A. D.; Campbell, J. A.; Alboaiji, S. F. K.; Muller, K. A.; Young, J.; Adamson, N.; Gascooke, J. R.; Jampaiah, D.; Sabri, Y. M.; Bhargava, S. K.; Ippolito, S. J.; Lewis, D. A.; Quinton, J. S.; Ellis, A. V.; Johs, A.; Bernardes, G. J. L.; Chalker, J. M. Laying Waste to Mercury: Inexpensive Sorbents Made from Sulfur and Recycled Cooking Oils. *Chem. Eur. J.* 2017, 23 (64), 16219–16230.
- (76) Hoefling, A.; Lee, Y. J.; Theato, P. Sulfur-Based Polymer Composites from Vegetable Oils and Elemental Sulfur: A Sustainable Active Material for Li-S Batteries. *Macromol. Chem. Phys.* **2017**, 218 (1), 1600303.
- (77) Parker, D. J.; Chong, S. T.; Hasell, T. Sustainable Inverse-Vulcanised Sulfur Polymers. RSC Adv. 2018, 8 (49), 27892–27899.
- (78) Mann, M.; Kruger, J. E.; Andari, F.; McErlean, J.; Gascooke, J. R.; Smith, J. A.; Worthington, M. J. H.; McKinley, C. C. C.; Campbell, J. A.; Lewis, D. A.; Hasell, T.; Perkins, M. V.; Chalker, J. M. Sulfur Polymer Composites as Controlled-Release Fertilisers. *Org. Biomol. Chem.* **2019**, *17* (7), 1929–1936.
- (79) Hoefling, A.; Nguyen, D. T.; Lee, Y. J.; Song, S.-W.; Theato, P. A Sulfur—Eugenol Allyl Ether Copolymer: A Material Synthesized via Inverse Vulcanization from Renewable Resources and Its Application in Li–S Batteries. *Mater. Chem. Front.* **2017**, *1* (9), 1818–1822.
- (80) Kang, H.; Kim, H.; Park, M. J. Sulfur-Rich Polymers with Functional Linkers for High-Capacity and Fast-Charging Lithium—Sulfur Batteries. *Adv. Energy Mater.* **2018**, 8 (32), 1802423.
- (81) Thiounn, T.; Lauer, M. K.; Bedford, M. S.; Smith, R. C.; Tennyson, A. G. Thermally-Healable Network Solids of Sulfur-Crosslinked Poly(4-Allyloxystyrene). *RSC Adv.* **2018**, 8 (68), 39074—39082.
- (82) Kim, E. T.; Chung, W. J.; Lim, J.; Johe, P.; Glass, R. S.; Pyun, J.; Char, K. One-Pot Synthesis of PbS NP/Sulfur-Oleylamine Copolymer Nanocomposites via the Copolymerization of Elemental Sulfur with Oleylamine. *Polym. Chem.* **2014**, *5* (11), 3617–3623.
- (83) Arslan, M.; Kiskan, B.; Cengiz, E. C.; Demir-Cakan, R.; Yagci, Y. Inverse Vulcanization of Bismaleimide and Divinylbenzene by Elemental Sulfur for Lithium Sulfur Batteries. *Eur. Polym. J.* **2016**, *80*, 70–77.
- (84) Arslan, M.; Kiskan, B.; Yagci, Y. Combining Elemental Sulfur with Polybenzoxazines via Inverse Vulcanization. *Macromolecules* **2016**, 49 (3), 767–773.
- (85) Shukla, S.; Ghosh, A.; Sen, U. K.; Roy, P. K.; Mitra, S.; Lochab, B. Cardanol Benzoxazine-Sulfur Copolymers for Li-S Batteries: Symbiosis of Sustainability and Performance. *ChemistrySelect* **2016**, *1* (3), 594–600.
- (86) Griebel, J. J.; Namnabat, S.; Kim, E. T.; Himmelhuber, R.; Moronta, D. H.; Chung, W. J.; Simmonds, A. G.; Kim, K.-J.; van der Laan, J.; Nguyen, N. A.; Dereniak, E. L.; Mackay, M. E.; Char, K.; Glass, R. S.; Norwood, R. A.; Pyun, J. New Infrared Transmitting Material via Inverse Vulcanization of Elemental Sulfur to Prepare High Refractive Index Polymers. *Adv. Mater.* **2014**, *26* (19), 3014–3018.
- (87) Liu, J.; Ueda, M. High Refractive Index Polymers: Fundamental Research and Practical Applications. *J. Mater. Chem.* **2009**, *19* (47), 8907–8919.
- (88) Kleine, T. S.; Nguyen, N. A.; Anderson, L. E.; Namnabat, S.; LaVilla, E. A.; Showghi, S. A.; Dirlam, P. T.; Arrington, C. B.; Manchester, M. S.; Schwiegerling, J.; Glass, R. S.; Char, K.; Norwood, R. A.; Mackay, M. E.; Pyun, J. High Refractive Index Copolymers with Improved Thermomechanical Properties via the Inverse Vulcanization of Sulfur and 1,3,5-Triisopropenylbenzene. *ACS Macro Lett.* **2016**, 5 (10), 1152–1156.
- (89) Bennett, H. E.; Guenther, A. H.; Milam, D.; Newnam, B. E. Laser-Induced Damage in Optical Materials: Fifteenth ASTM Symposium. *Appl. Opt.* **1986**, 25 (2), 258–275.

- (90) Griebel, J. J.; Nguyen, N. A.; Astashkin, A. V.; Glass, R. S.; Mackay, M. E.; Char, K.; Pyun, J. Preparation of Dynamic Covalent Polymers via Inverse Vulcanization of Elemental Sulfur. *ACS Macro Lett.* **2014**, 3 (12), 1258–1261.
- (91) Griebel, J. J.; Nguyen, N. A.; Namnabat, S.; Anderson, L. E.; Glass, R. S.; Norwood, R. A.; Mackay, M. E.; Char, K.; Pyun, J. Dynamic Covalent Polymers via Inverse Vulcanization of Elemental Sulfur for Healable Infrared Optical Materials. *ACS Macro Lett.* **2015**, 4 (9), 862–866.
- (92) Burnett, J. H.; Kaplan, S. G.; Stover, E.; Phenis, A. Refractive Index Measurements of Ge. *Infrared Sensors, Devices, and Applications VI*; Proceedings of SPIE, San Diego, 2016, 99740X, 1–11.
- (93) Eisenberg, A.; Tobolsky, A. V. Equilibrium Polymerization of Selenium. J. Polym. Sci. 1960, 46 (147), 19–28.
- (94) Boyd, D. A.; Baker, C. C.; Myers, J. D.; Nguyen, V. Q.; Drake, G. A.; McClain, C. C.; Kung, F. H.; Bowman, S. R.; Kim, W.; Sanghera, J. S. ORMOCHALCs: Organically Modified Chalcogenide Polymers for Infrared Optics. *Chem. Commun.* **2017**, 53 (1), 259–262.
- (95) Anderson, L. E.; Kleine, T. S.; Zhang, Y.; Phan, D. D.; Namnabat, S.; LaVilla, E. A.; Konopka, K. M.; Ruiz Diaz, L.; Manchester, M. S.; Schwiegerling, J.; Glass, R. S.; Mackay, M. E.; Char, K.; Norwood, R. A.; Pyun, J. Chalcogenide Hybrid Inorganic/Organic Polymers: Ultrahigh Refractive Index Polymers for Infrared Imaging. ACS Macro Lett. 2017, 6 (5), 500–504.
- (96) Gomez, I.; Mantione, D.; Leonet, O.; Blazquez, J. A.; Mecerreyes, D. Hybrid Sulfur–Selenium Co-Polymers as Cathodic Materials for Lithium Batteries. *ChemElectroChem* **2018**, *5* (2), 260–265.
- (97) Pavlichenko, I.; Broda, E.; Fukuda, Y.; Szendrei, K.; Hatz, A. K.; Scarpa, G.; Lugli, P.; Bräuchle, C.; Lotsch, B. V. Bringing One-Dimensional Photonic Crystals to a New Light: An Electrophotonic Platform for Chemical Mass Transport Visualisation and Cell Monitoring. *Mater. Horiz.* **2015**, *2* (3), 299–308.
- (98) Canazza, G.; Scotognella, F.; Lanzani, G.; De Silvestri, S.; Zavelani-Rossi, M.; Comoretto, D. Lasing from All-Polymer Microcavities. *Laser Phys. Lett.* **2014**, *11* (3), 35804.
- (99) Kleine, T. S.; Diaz, L. R.; Konopka, K. M.; Anderson, L. E.; Pavlopolous, N. G.; Lyons, N. P.; Kim, E. T.; Kim, Y.; Glass, R. S.; Char, K.; Norwood, R. A.; Pyun, J. One Dimensional Photonic Crystals Using Ultrahigh Refractive Index Chalcogenide Hybrid Inorganic/Organic Polymers. ACS Macro Lett. 2018, 7 (7), 875–880. (100) Boyd, D. A.; Nguyen, V. Q.; McClain, C. C.; Kung, F. H.; Baker, C. C.; Myers, J. D.; Hunt, M. P.; Kim, W.; Sanghera, J. S. Optical Properties of a Sulfur-Rich Organically Modified Chalcogenide Polymer Synthesized via Inverse Vulcanization and Containing an Organometallic Comonomer. ACS Macro Lett. 2019, 8 (2), 113–116.
- (101) Lee, J. M.; Noh, G. Y.; Kim, B. G.; Yoo, Y.; Choi, W. J.; Kim, D.-G.; Yoon, H. G.; Kim, Y. S. Synthesis of Poly(Phenylene Polysulfide) Networks from Elemental Sulfur and p-Diiodobenzene for Stretchable, Healable, and Reprocessable Infrared Optical Applications. ACS Macro Lett. 2019, 8 (8), 912–916.
- (102) Fagerburg, D. R.; Van Sickle, D. E. Reaction Condition Effects in the Melt Preparation of Poly(Phenylene Sulfide) from p-Iodophenyl Disulfide. *J. Appl. Polym. Sci.* **1994**, *51* (6), 989–997.
- (103) Rule, M.; Fagerburg, D. R.; Watkins, J. J.; Lawrence, P. B.; Zimmerman, R. L.; Cloyd, J. D. Some Characteristics of a New and Novel Melt Preparation Method for Poly(Phenylene Sulfide). *Makromol. Chem., Macromol. Symp.* 1992, 54–55 (1), 233–246.
- (104) Nam, K.-H.; Lee, A.; Lee, S.-K.; Hur, K.; Han, H. Infrared Transmitting Polyimides Based on Chalcogenide Element-Blocks with Tunable High-Refractive Indices and Broad Optical Windows. *J. Mater. Chem. C* **2019**, *7* (34), 10574–10580.
- (105) NIST Mass Spectrometry Data Center, Wallace, W. E. Infrared Spectra. In *NIST Chemistry WebBook*, NIST Standard Reference Database Number 69; Linstrom, P. J., Mallard, W. G., Eds.; National Institute of Standards and Technology: Gaithersburg, MD, 2018.

(106) Kleine, T. S.; Lee, T.; Carothers, K. J.; Hamilton, M. O.; Anderson, L. E.; Ruiz Diaz, L.; Lyons, N. P.; Coasey, K. R.; Parker, W. O.; Borghi, L.; Mackay, M. E.; Char, K.; Glass, R. S.; Lichtenberger, D. L.; Norwood, R. A.; Pyun, J. Infrared Fingerprint Engineering: A Molecular Design Approach to Long Wave Infrared Transparency with Polymeric Materials. *Angew. Chem., Int. Ed.* **2019**, *58*, 17656–17660.